Wide-Area Oscillation Damping in Low-Inertia Grids under Time-Varying Communication Delays

Sultan Alghamdi*, Uros Markovic†, Ognjen Stanojev†, Johannes Schiffer‡, Gabriela Hug†, and Petros Aristidou*
* School of Electronic and Electrical Engineering, University of Leeds, Leeds, UK
† EEH - Power Systems Laboratory, ETH Zurich, Zurich, Switzerland
‡ Institute of Electrical and Thermal Energy Systems, Brandenburg University of Technology Cottbus-Senftenberg, Germany

***Abstract*—Wide-Area Control (WAC) can be efficiently used for oscillation damping in power systems. However, to implement a WAC, a communication network is required to transmit signals between the generation units and the control center. In turn, this makes WAC vulnerable to time-varying communication delays that, if not appropriately considered in the control design, can destabilize the system. Moreover, with the increasing integration of renewable energy resources into the grid, usually interfaced via power electronics, power system dynamics are becoming drastically faster and making WAC more vulnerable to communication delays. In this paper, we propose a design procedure for a delay-robust wide-area oscillation damping controller for low-inertia systems. Its performance is illustrated on the well-known Kundur two-area system. The results indicate that the obtained WAC successfully improves the oscillation damping while ensuring robustness against time-varying communication delays.**

***Index Terms*—Low-inertia systems, oscillation damping, time-varying communication delay, wide-area control.**

I. Introduction

A. Motivation and Related Work

Electric power systems are frequently subjected to low-frequency inter-area oscillations caused by Synchronous Generators (SGs), or coherent groups of generators, oscillating against each other in an interconnected system [1]. Insufficient damping of such oscillations can lead to increased losses, excessive strain on the mechanical components of generators, and in extreme cases instability. Traditionally, these under-damped oscillations have been addressed by deploying decentralized controllers called Power System Stabilizers (PSSs) at units participating in the power swing modes. Various control strategies for tuning of PSS parameters have been proposed in the literature, such as pole placement [2], root locus [3], $\mathcal{H}_2$ [4] and $\mathcal{H}_\infty$ [5] norm. In particular, PSSs can improve oscillation damping by adjusting the reference signal of the exciter, thus counteracting a high-gain fast response of Automatic Voltage Regulators (AVRs). Nevertheless, relying solely on decentralized control might sometimes be inadequate for providing sufficient damping of inter-area modes, or even worsen the performance of the overall system [6], [7]. Recently, with the advancements in Wide-Area Monitoring and Control (WAMC), new methods have been proposed that exploit WAMC capabilities to improve damping by coordinating multiple units through a wide-area controller [8], [9].

The deployment of a communication network to enable WAMC is however not problem-free and can introduce additional vulnerabilities to the system, one of the most prominent being communication delays. The latter arise in the form of transmission delays, propagation delays, processing delays and queuing delays [10], [11]. Since the presence of communication delays influences the system performance and can even lead to instability [12], taking such delays into account is necessary in order to design a well-functioning WAC.

While this problem has already been investigated for constant delays in the frequency domain [13], [14], the proposed analyses are not applicable to the case of time-varying delays. Yet, the latter are ubiquitous in sampled data networked control systems [15], [16], such as WAMC. The underlying reasons are the joint presence of digital controls and continuous physical dynamics as well as the fact that network access and propagation delays typically depend on the communication network congestion and are, hence, time-varying [17]. Therefore, following standard practice in sampled-data and networked control systems, in the present work the communication delays are represented by bounded, time-dependent functions [15], [16]. As a consequence, the resulting dynamical system is non-autonomous, which implies that an eigenvalue-based stability analysis is inconclusive [18]. A standard alternative is to employ the Lyapunov-Krasovskii theory in combination with a Linear Matrix Inequality (LMI) approach [15], [16]. This has been pursued for WAC synthesis in power systems with purely conventional generation in [19]–[22].

Current developments in power systems, driven by environmental incentives, lead to the displacement of conventional SGs by Renewable Energy Sources (RESs). Renewable generators are usually interfaced to the grid via power electronic converters, which operate on drastically shorter timescales and electrically decouple the kinetic inertia stored in rotating masses of the RES generators from the network. As a result, the voltage and frequency dynamics, as well as the respective control interaction in low-inertia systems, become more complex and harder to analyze [23]. Moreover, with the displacement of SGs the number of PSSs providing oscillation damping is also reduced. This issue was partially addressed in [24] with the development of a global model predictive controller for providing power-oscillation damping and stabilization of large AC power systems using Voltage Source Converter (VSC)-based HVDC links. On the other hand, employing RESs for participation in the inter-area oscillation damping has been considered in [25]–[27]. However, none

of the above studies considers time-varying communication delays in the WACs.

B. Contribution

The main contribution is a design procedure for a delay-robust, wide-area output feedback controller that regulates both conventional and converter-based generators to enhance oscillation damping in a low-inertia system with detailed dynamics and under the consideration of time-varying delays.

Compared to the existing work on WAC where full state feedback controllers were used [8], [9], [28], we propose a static output feedback controller which eases its practical implementation. Moreover, the proposed control synthesis ensures damping of low-frequency modes by minimizing the upper-bound of the L_2-gain, which is equivalent to the $\mathcal{H}_\infty$ norm of a linear time-invariant system [16], [18] and has been proven to be effective in improving the damping of inter-area modes [5], [9], [19], [29], [30]. For this purpose and, as in any practical WAMC there will inevitably be a minimum nonzero communication delay, we model the delays as interval time-varying delays, i.e., assuming non-zero constant upper and lower bounds [16]. The control synthesis is derived by applying the augmented Lyapunov-Krasovskii functional (LKF) in [31] together with the descriptor method. Subsequently, the variable transformation from [32] is employed to formulate the control design problem as a convex optimization problem with LMI constraints. A similar approach is employed in [33] for designing a secondary frequency controller in microgrids.

The remainder of this paper is structured as follows. In Section II, the detailed dynamic model of a low-inertia system is introduced together with the model reduction approach based on first-order singular perturbation for alleviating the system complexity pertaining to several distinctive timescales. Section III presents a control synthesis approach for designing the WAC that ensures robustness with respect to time-varying communication delays. The effectiveness of the proposed procedure is validated on the Kundur two-area system in Section IV. Finally, a brief summary and potential directions for future work are provided in Section V.

II. Power System Modeling

A. VSC Control Scheme

In this work, we consider a state-of-the-art, *grid-forming* VSC control scheme previously described in [34], where the converter is operated as a Virtual Synchronous Machine (VSM). In particular, the outer control loop comprises the active and reactive power controllers that compute the output voltage angle and magnitude references by adjusting the pre-defined setpoints according to a measured power imbalance. Subsequently, the reference voltage vector signal is passed through a virtual impedance block as well as the inner control loop consisting of cascaded voltage and current PI controllers. The output is combined with the DC-side voltage in order to generate the pulse-width modulation signal. Due to a grid-forming mode of operation, a synchronization unit - usually in the form of a Phase-Locked Loop (PLL) - is omitted from the design. With inclusion of the filter current and voltage dynamics, the complete mathematical model comprises 13 state variables and is implemented in a rotating (dq)-frame and per unit. More details on the overall converter control structure, employed parametrization, potential operation modes and respective transient properties can be found in [23], [34], [35].

B. Synchronous Generator Model

For synchronous generators we consider a round rotor model equipped with a prime mover and a *TGOV1* governor. An AVR, based on a simplified excitation system *SEXS*, is incorporated for the purpose of voltage regulation, together with a *PSS1A* power system stabilizer. Detailed control configuration and tuning parameters are provided in [36]. The internal machine dynamics are characterized by the flux linkage transients in the rotor circuit (field winding, two damper windings in the q-axis and one in the d-axis), as transients in the stator windings decay rapidly and can thus be neglected. The inclusion of the swing equation dynamics and stator circuit balance completes the respective set of Differential-Algebraic Equations (DAEs). The SG is interfaced to the grid through a transformer and modeled in the Synchronously-rotating Reference Frame (SRF). Internal machine dynamics, combined with six controller states pertaining to governor, AVR and PSS, as well as the electrical circuit interface yield a 14^{th}-order system. For more details regarding the SG modeling and internal parameter computation we refer the reader to [1].

C. Transmission Network Dynamics

The transmission network comprises transmission lines modeled as π-sections. Moreover, loads are modeled as constant impedance RL loads. In order to represent all system variables in a common SRF, following standard practice [37], [38], the terminal currents and voltages of each generator unit are mapped to the respective network nodes with generator connection, and subsequently aligned to the uniform SRF of an arbitrary synchronous generator or a grid-forming inverter. Finally, the line dynamics are captured using a conventional DAE representation of an RLC circuit. The exact mathematical formulation and the appropriate SRF alignment are presented in [23].

D. Model-Order Reduction

Combining the network model with the individual generator dynamics completes the set of Ordinary-Differential Equations (ODEs). The linearized model is thus defined in the general state-space form as:

$$\dot{\bar{x}} = \bar{A}\bar{x} + \bar{B}u, \tag{1}$$

where $\bar{x} \in \mathbb{R}^k$ is the state variable vector, $u \in \mathbb{R}^m$ is the input vector, and $\bar{A} \in \mathbb{R}^{k\times k}$ and $\bar{B} \in \mathbb{R}^{k\times m}$ are constant matrices.

Conventional power systems are characterized by relatively slow voltage and frequency controllers due to large turbine and governor time constants of SGs (in the range of seconds). However, with the inclusion of fast-acting, converter-based generation, the system dynamics become more complex. More

precisely, the time constants of the PI controllers and low-pass filters associated with the inner and outer inverter control loops are one or two orders of magnitude smaller than the ones of the SGs. Moreover, the transmission line dynamics, traditionally neglected in SG-based power system analysis due to timescale separation, become significant in low-inertia grids [23]. However, such dynamical systems experience a wide range of time constants, which increases model complexity and might lead to an ill-conditioned matrix $\bar{A}$.

The issues pertaining to tractability are resolved by employing a model-order reduction based on a first-order singular perturbation [39], [40]. Let us consider a system with a distinct timescale separation between the fast and slow dynamics, which allows us to rewrite the formulation in (1) as

$$\dot{x}_s = A_{ss}x_s + A_{sf}x_f + B_s u, \tag{2a}$$
$$\Upsilon \dot{x}_f = A_{fs}x_s + A_{ff}x_f + B_f u, \tag{2b}$$

where the subscripts s and f correspond to slow and fast states respectively, and Υ is a set of parameters designating the fast dynamics. Unlike in the traditional zero-order approach, where fast dynamics are completely neglected by converting the corresponding differential equations into algebraic ones, the first-order method removes the fast states by stating that the first derivative of x_f is non-zero, whereas the second derivative is negligible. This property is especially useful in systems with several distinctive timescales and has a potential of better capturing the impact of fast states on slow system dynamics. Inserting such a dependence in (2b) and separating different orders of magnitude yields a first-order ODE system of the form [39], [40]:

$$\dot{x}_s = Ax_s + B_u u, \tag{3a}$$

where

$$A = \left(I + A_{sf}A_{ff}^{-1}\Upsilon A_{ff}^{-1}A_{fs}\right)^{-1}\left(A_{ss} - A_{sf}A_{ff}^{-1}A_{fs}\right), \tag{3b}$$
$$B_u = \left(I + A_{sf}A_{ff}^{-1}\Upsilon A_{ff}^{-1}A_{fs}\right)^{-1}\left(B_s - A_{sf}A_{ff}^{-1}B_f\right) \tag{3c}$$

are the reduced state-space matrices and $x_s \in \mathbb{R}^n$ denotes the preserved slow states of interest. Understandably, the reduced-order model is only valid if A_{ff} and $I + A_{sf}A_{ff}^{-1}\Upsilon A_{ff}^{-1}A_{fs}$ are nonsingular.

The proposed first-order method is employed for eliminating the electrical states of the converter, corresponding to filter current and voltage dynamics, as well as the flux linkage dynamics of the synchronous generator. By removing these fast states we obtain a 9^{th}-order VSC model and a 10^{th}-order SG model, which compared to the original system (1) exhibit lower complexity and, in the authors' experience, result in significantly better-conditioned system matrices [41].

III. Delay-robust wide-area control design

We now investigate the following linear MIMO system:

$$\dot{x}_s = Ax_s + B_u\, u + B_w\, w, \tag{4a}$$
$$y = C_y\, x_s, \tag{4b}$$
$$z = C_z\, x_s + D_u\, u + D_w\, w, \tag{4c}$$

where $x_s \in \mathbb{R}^n$ is the state variable vector, $u \in \mathbb{R}^m$ is the input vector, $w(t) \in L_2[0,\infty)$[1] is the external disturbance vector, $y \in \mathbb{R}^q$ is the output vector, $z \in \mathbb{R}^p$ is the performance output vector, $A \in \mathbb{R}^{n\times n}$, $B_u \in \mathbb{R}^{n\times m}$, $B_w \in \mathbb{R}^{n\times w}$, $C_y \in \mathbb{R}^{q\times n}$, $C_z \in \mathbb{R}^{p\times n}$, $D_u \in \mathbb{R}^{p\times m}$, and $D_w \in \mathbb{R}^{p\times w}$ are constant matrices. We assume that the pair (A, B_u) is stabilizable.

A. Controller Structure

We consider the following static output feedback controller for the system (4):

$$u = -Ky = -KC_y\, x_s, \tag{5}$$

where $K \in \mathbb{R}^{m\times q}$ is the controller gain to be designed. The controller (5) is simpler and easier for practical implementation than a full state feedback controller since it only requires the system output to be measurable.

With regard to the communication delays, we assume that the information flow from the i-th node to the WAMC center and vice versa is affected by a fast, time-varying, bounded, communication interval delay $\tau : \mathbb{R}_{\geq 0} \to [h_1, h_2]$, $h_1 \in \mathbb{R}_{\geq 0}$, $h_2 \in \mathbb{R}_{>0}$, $h_2 > h_1$ (where h_1 and h_2 are the lower and upper communication delay limits, respectively). For clarity of exposition we assume uniform delays. However, the proposed approach presented can be extended to heterogeneous delays at the expense of a more involved notation, see e.g. [42]–[44]. Hence, the closed-loop system is obtained by combining (4) with the delayed variant of (5), i.e.,

$$\dot{x}_s = Ax_s - B_uKC_y\, x_s(t-\tau(t)) + B_w w, \tag{6a}$$
$$z = C_z x_s - D_uKC_y\, x_s(t-\tau(t)) + D_w w. \tag{6b}$$

The objective of damping the inter-area modes is considered in our approach by minimizing the L_2-gain $\gamma \in \mathbb{R}_{>0}$ of (6), which is defined as the maximum energy amplification ratio between the disturbance input signal w and the performance output signal z [16], [18]. For instance, defining the output performance matrix C_z in (6), such that z represents the frequencies of the generation units and then minimizing the L_2-gain γ, should reduce the frequency oscillations in the system following a disturbance w. The control design objectives are summarized in the following problem statement.

Problem III.1. *Consider the system* (4). *Given* $h_1 \in \mathbb{R}_{\geq 0}$, $h_2 \in \mathbb{R}_{\geq 0}$ *with* $h_1 \leq \tau(t) \leq h_2$, *design a static output feedback controller* (5)*, such that the origin is a uniformly asymptotically stable equilibrium point of the resulting closed-loop system* (6) *and its* L_2 *gain is minimized.*

[1] A signal $u : \mathbb{R}_{\geq 0} \to \mathbb{R}^m$ is in L_2 if its L_2-norm $\|u\|_{L_2}$, given by

$$\|u\|_{L_2} = \sqrt{\int_0^\infty u^\top(t)u(t)dt}$$

is finite [18].

B. Main Result

We provide the following solution to Problem III.1.

Proposition III.2. *Consider the system* (6). *Fix* $h_1 \geq 0$, *and* $h_2 > h_1$. *Suppose that there exists a parameter* $\bar{\gamma} > 0$ *and matrices* $\bar{P} \in \mathbb{R}^{3n\times 3n}_{>0}$, $\bar{R}_1 \in \mathbb{R}^{n\times n}_{>0}$, $\bar{R}_2 \in \mathbb{R}^{n\times n}_{>0}$, $\bar{S}_1 \in \mathbb{R}^{n\times n}_{>0}$, $\bar{S}_2 \in \mathbb{R}^{n\times n}_{>0}$, $M \in \mathbb{R}^{q\times q}$, $N \in \mathbb{R}^{m\times q}$, $W \in \mathbb{R}^{n\times n}$, *and* $\bar{X} \in \mathbb{R}^{2n\times 2n}$, *such that the following problem is feasible:*

$$\begin{aligned} &\min \bar{\gamma} \\ &\textit{subject to} \\ &\begin{bmatrix} \bar{\psi}_1(h_1) & \bar{\psi}_2 \\ * & -I \end{bmatrix} < 0, \qquad \begin{bmatrix} \bar{\psi}_1(h_2) & \bar{\psi}_2 \\ * & -I \end{bmatrix} < 0, \qquad (7) \\ &\bar{\psi}_3 = \begin{bmatrix} \tilde{R}_2 & \bar{X} \\ * & \tilde{R}_2 \end{bmatrix} \geq 0, \qquad MC_y = C_y W, \end{aligned}$$

where

$$\begin{aligned} h_{12} &= h_2 - h_1,\ \tilde{R}_2 = diag(\bar{R}_2, 3\bar{R}_2),\ \Gamma = [G_2^\top, G_3^\top]^\top, \\ \bar{\psi}_1(\tau) &= \bar{\psi}_{11} + G_0^\top \bar{P} G_1(\tau) + G_1^\top(\tau) \bar{P} G_0 - \Gamma^\top \bar{\psi}_3 \Gamma, \\ \bar{\psi}_2^\top &= [C_z W, \mathbb{0}, \mathbb{0}, -D_u N C_y, \mathbb{0}, \mathbb{0}, \mathbb{0}, \mathbb{0}, D_w], \\ G_0 &= \begin{bmatrix} \mathbb{0} & I & \mathbb{0} & \mathbb{0} & \mathbb{0} & \mathbb{0} & \mathbb{0} & \mathbb{0} & \mathbb{0} \\ I & \mathbb{0} & -I & \mathbb{0} & \mathbb{0} & \mathbb{0} & \mathbb{0} & \mathbb{0} & \mathbb{0} \\ \mathbb{0} & \mathbb{0} & I & \mathbb{0} & -I & \mathbb{0} & \mathbb{0} & \mathbb{0} & \mathbb{0} \end{bmatrix}, \\ G_1(\tau) &= \begin{bmatrix} I & \mathbb{0} & \mathbb{0} & \mathbb{0} & \mathbb{0} & \mathbb{0} & \mathbb{0} & \mathbb{0} & \mathbb{0} \\ \mathbb{0} & \mathbb{0} & \mathbb{0} & \mathbb{0} & \mathbb{0} & h_1 I & \mathbb{0} & \mathbb{0} & \mathbb{0} \\ \mathbb{0} & \mathbb{0} & \mathbb{0} & \mathbb{0} & \mathbb{0} & \mathbb{0} & (\tau - h_1) I & (h_2 - \tau) I & \mathbb{0} \end{bmatrix}, \\ G_2 &= \begin{bmatrix} \mathbb{0} & \mathbb{0} & I & -I & \mathbb{0} & \mathbb{0} & \mathbb{0} & \mathbb{0} & \mathbb{0} \\ \mathbb{0} & \mathbb{0} & I & I & \mathbb{0} & \mathbb{0} & -2I & \mathbb{0} & \mathbb{0} \end{bmatrix}, \\ G_3 &= \begin{bmatrix} \mathbb{0} & \mathbb{0} & \mathbb{0} & I & -I & \mathbb{0} & \mathbb{0} & \mathbb{0} & \mathbb{0} \\ \mathbb{0} & \mathbb{0} & \mathbb{0} & I & I & \mathbb{0} & \mathbb{0} & -2I & \mathbb{0} \end{bmatrix}, \end{aligned}$$

and $\bar{\psi}_{11}$ *is given in* (10). *Choose the controller gain as*

$$K = NM^{-1}. \qquad (11)$$

Then, for all $\tau(t) \in [h_1, h_2]$, *the origin is a uniformly asymptotically stable equilibrium point of the system* (6) *and the system has an* L_2*-gain less than or equal to* $\gamma = \sqrt{\bar{\gamma}}$.

The proof is given in the Appendix.

IV. Numerical Example

The performance of the proposed WAC is assessed using the Kundur two-area system [1], which is prone to local and inter-area oscillations. The system consists of two weakly connected areas, with each comprising two generators. The parameters of the system are given in [1, Example 12.6]. Furthermore, three system configurations are considered in this work: (1) an all SG-based system serving as a benchmark for the effectiveness of the proposed WAC; (2) each area contains a mix of synchronous and converter-based generation, as illustrated in Fig. 1; and (3) Area 1 is all SG-based and Area 2 converter-based.

Preliminary investigations using modal analysis show the presence of underdamped, low-frequency modes in all three configurations. Table I lists the main eigenvalues as well as

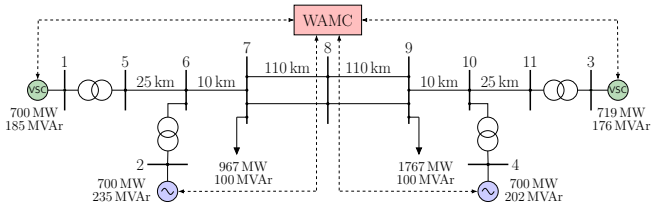

Fig. 1. Topology of the investigated Kundur two-area system with WAC (*Left: Area 1, Right: Area 2*).

TABLE I
Underdamped Modes of the Kundur Two-Area System

Config.	Eigenvalues	Damping ratio	Frequency [Hz]	Mode type
1	$-0.0846 \pm 4.82i$	0.0176	0.76712	Local
	$-0.0913 \pm 4.82i$	0.019	0.76714	Local
	$-0.142 \pm 4.04i$	0.035	0.6434	Inter-area
2	$-0.228 \pm 4.46i$	0.0511	0.7098	Inter-area
3	$-0.0846 \pm 4.82i$	0.0176	0.76714	Local

the damping ratios and natural frequencies of these modes. Moreover, Fig. 2 illustrates the mode shape [1] of these modes. It also suggests that the first configuration exhibits two local low-frequency modes and one inter-area mode, while the second and third configuration are prone to one inter-area and one local mode, respectively. All of the underdamped modes and the effectiveness of the proposed WAC are studied in the subsequent time-domain analysis.

Next, to design the WAC for all considered configurations, we solve the optimization problem (7). We assume that the exchanged information via a communication network is affected by fast-varying, uniform interval delays with $h_1 = 80\,\text{ms} \leq \tau(t) \leq h_2 = 140\,\text{ms}$. Furthermore, we set $D_u = D_w = 0$ and choose $C_y = C_z$ such that the output y in (4) and the performance output z in (6) describe the frequencies. The implementation is done in MATLAB (R2018b), using Yalmip (version 09-02-2018) [45] and the solver MOSEK (version 8.1.0.51) [46]. To simulate the

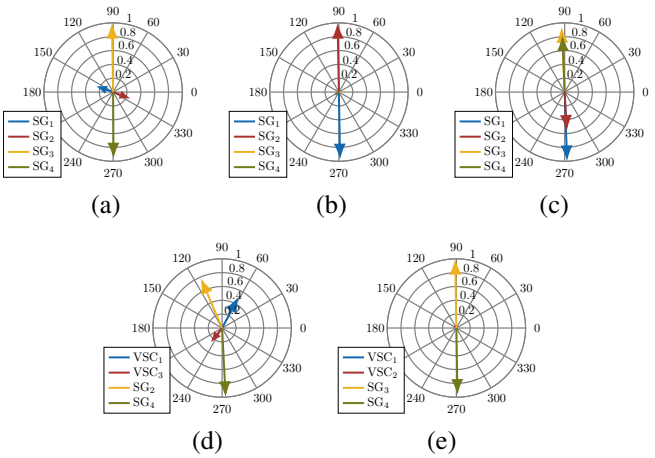

Fig. 2. Mode shape of underdamped modes. Configuration 1: (a) mode 1, (b) mode 2, (c) mode 3; (d) Configuration 2; (e) Configuration 3. Note that VSC_i and SG_i denote the respective generator types connected at node i.

$$\bar{\psi}_{11}=\begin{bmatrix} AW+WA^\top+\bar{S}_1-4\bar{R}_1 & -W+\epsilon WA^\top & -2\bar{R}_1 & -B_uNC_y & \mathbb{0} & 6\bar{R}_1 & \mathbb{0} & \mathbb{0} & B_w \\ * & -2\epsilon W+h_1^2\bar{R}_1+h_{12}^2\bar{R}_2 & \mathbb{0} & -\epsilon B_uNC_y & \mathbb{0} & \mathbb{0} & \mathbb{0} & \mathbb{0} & \epsilon B_w \\ * & * & -\bar{S}_1+\bar{S}_2-4\bar{R}_1 & \mathbb{0} & \mathbb{0} & 6\bar{R}_1 & \mathbb{0} & \mathbb{0} & \mathbb{0} \\ * & * & * & \mathbb{0} & \mathbb{0} & \mathbb{0} & \mathbb{0} & \mathbb{0} & \mathbb{0} \\ * & * & * & * & -\bar{S}_2 & \mathbb{0} & \mathbb{0} & \mathbb{0} & \mathbb{0} \\ * & * & * & * & * & -12\bar{R}_1 & \mathbb{0} & \mathbb{0} & \mathbb{0} \\ * & * & * & * & * & * & \mathbb{0} & \mathbb{0} & \mathbb{0} \\ * & * & * & * & * & * & * & \mathbb{0} & \mathbb{0} \\ * & * & * & * & * & * & * & * & -\bar{\gamma}I \end{bmatrix} \tag{10}$$

communication delays, we employ the transition and variable time delay blocks in MATLAB/SIMULINK with a sampling time of $T_s = 2\,\text{ms}$.

We first investigate Configuration 1, i.e., a power system comprised solely of SGs. This allows us to evaluate the performance of the proposed control synthesis in a conventional power system. The comparison between an uncontrolled (open-loop) system, with only PSS participating in oscillation damping, and the system with WAC and communication delays is conducted. The simulation results given in Fig. 3 clearly indicate that the groups of generators in two areas oscillate against each other. On the other hand, designing the WAC using Proposition III.2 reduces the system's L_2-gain from $\gamma = 2.2078$ (without the WAC) to $\gamma = 1.3425$ (with the WAC), while ensuring robustness against communication delays. As can be seen from Fig. 3 this also results in a significant reduction of the oscillations.

Similarly, Fig. 4 shows the results of the same test case for a low-inertia grid with Configuration 2. We first investigate the open-loop behavior of the system, followed by the response with the WAC and including time-varying communication delays. The results confirm that the uncontrolled system exhibits oscillations between the two-areas, even if two of the generators are converter-based. The WAC implementation of the static feedback control gain K improves the system behavior by reducing the L_2-gain from $\gamma = 3.019$ (without the WAC) to $\gamma = 1.7963$ (with the WAC), which effectively damps the oscillations and, in addition, guarantees delay-robustness.

Finally, in Configuration 3 we split the generation types between the two areas. As a result, there are no inter-area modes between the all inverter-based and the all SG-based areas. In fact, the grid-forming inverters are synchronized and their frequency response is very well damped. Nonetheless, the local oscillations between the SGs in Area 2 are still present, as illustrated in Fig. 5. Applying the WAC design can also improve these oscillation by means of reducing the system's L_2-gain. The designed WAC reduces the L_2-gain from $\gamma = 2.0628$ (without the WAC) to $\gamma = 1.0965$ (with the WAC). Figure 5 shows that the controller significantly improves the damping of local oscillation.

The three configurations investigated above show the effectiveness of the proposed delay-robust WAC. More precisely, in Configurations 1 and 2 the proposed controller successfully damps the inter-area oscillations, even in the presence of

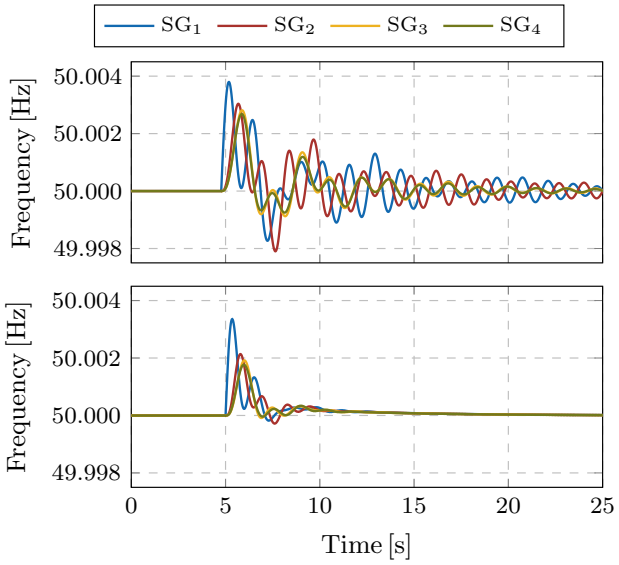

Fig. 3. Configuration 1 - frequency response of a traditional power system after a step-change in load for two different scenarios: (i) uncontrolled system; (ii) controlled system with communication delays.

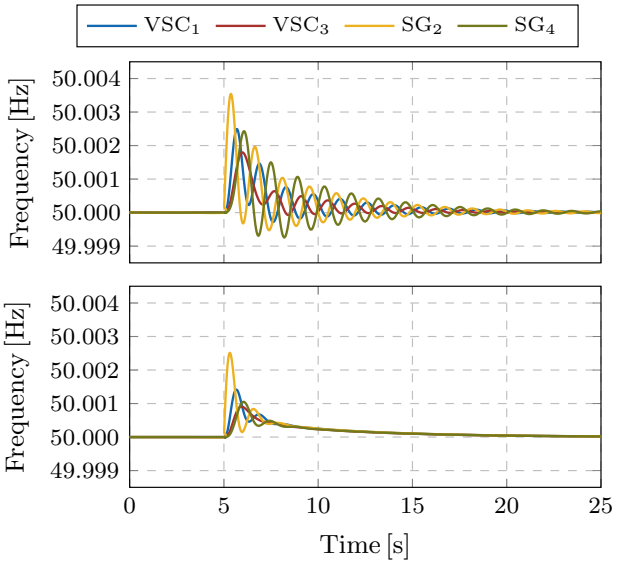

Fig. 4. Configuration 2 - frequency response of a low-inertia system after a step-change in load for two different scenarios: (i) uncontrolled system; (ii) controlled system with communication delays.

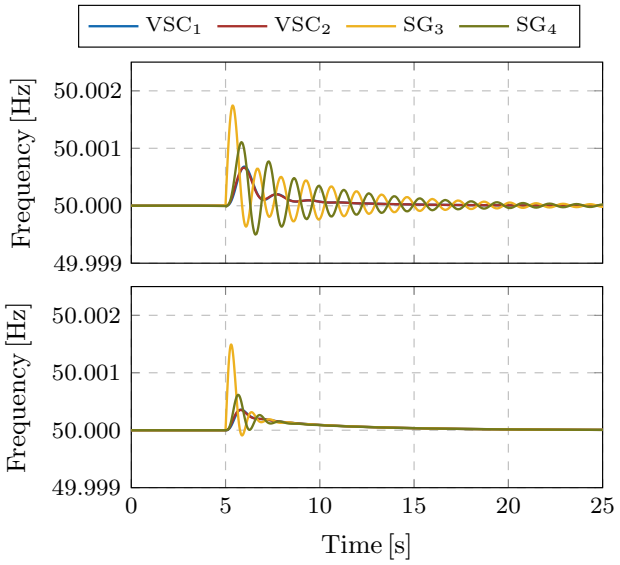

Fig. 5. Configuration 3 - frequency response of a low-inertia system after a step-change in load for two different scenarios: (i) uncontrolled system; (ii) controlled system with communication delays.

time-varying delays. Furthermore, since the controller aims to minimize the L_2-gain of the system, it also exhibits the ability to damp local oscillations, as shown in Configuration 3.

V. Conclusions

In this work, we investigate the problem of wide-area oscillation damping control in low-inertia systems in the presence of time-varying communication delays. We address these challenges by proposing a design procedure for a WAC that guarantees delay-robustness and simultaneously minimizes the L_2 gain of the system. More precisely, we consider a detailed model of a low-inertia system and combine an augmented LKF with the descriptor method and a change of control variables to develop a static output feedback controller synthesis. Furthermore, the proposed control design is tested on the Kundur two-area system. The results demonstrate that the proposed approach successfully improves oscillation damping and ensures robustness with respect to time-varying communication delays.

In future work, we plan to extend the study by applying the proposed controller synthesis to large-scale low-inertia systems. In addition, we intend to introduce a sparsity-promoting feature in the control design, in order to reduce the required information exchange of the WAC.

References

[1] P. Kundur, *Power system stability and control*. McGraw-Hill, 1994.
[2] H. Othman, J. J. Sanchez-Gasca, M. A. Kale, and J. H. Chow, "On the design of robust power system stabilizers," in *Proc. of the 28th IEEE CDC*, 1989, pp. 1853–1857 vol.2.
[3] M. Klein, G. J. Rogers, S. Moorty, and P. Kundur, "Analytical investigation of factors influencing power system stabilizers performance," *IEEE Trans. Energy Convers.*, vol. 7, no. 3, pp. 382–390, 1992.
[4] A. Mešanović, U. Münz, and C. Heyde, "Comparison of $\mathcal{H}_\infty$, $\mathcal{H}_2$, and pole optimization for power system oscillation damping with remote renewable generation," *IFAC*, vol. 49, no. 27, pp. 103 – 108, 2016.
[5] A. Mešanović, D. Unseld, U. Münz, C. Ebenbauer, and R. Findeisen, "Parameter tuning and optimal design of decentralized structured controllers for power oscillation damping in electrical networks," in *ACC*, 2018, pp. 3828–3833.
[6] I. Kamwa, J. Beland, G. Trudel, R. Grondin, C. Lafond, and D. McNabb, "Wide-area monitoring and control at hydro-quebec: past, present and future," in *IEEE PES General Meeting*, 2006.
[7] G. J. Rogers, "The application of power system stabilizers to a multi-generator plant," *IEEE Trans. Power Syst.*, vol. 15, pp. 350–355, 2000.
[8] F. Dörfler, M. R. Jovanović, M. Chertkov, and F. Bullo, "Sparsity-promoting optimal wide-area control of power networks," *IEEE Trans. Power Syst.*, vol. 29, no. 5, pp. 2281–2291, 2014.
[9] S. Schuler, U. Münz, and F. Allgöwer, "Decentralized state feedback control for interconnected systems with application to power systems," *Journal of Process Control*, vol. 24, no. 2, pp. 379–388, 2014.
[10] Y. Wang, P. Yemula, and A. Bose, "Decentralized communication and control systems for power system operation," *IEEE Trans. Smart Grid*, vol. 6, no. 2, pp. 885–893, 2015.
[11] P. Kansal and A. Bose, "Smart grid communication requirements for the high voltage power system," in *IEEE PES General Meeting*, 2011.
[12] Y. Ghaedsharaf, C. Somarakis, F. Dörfler, and N. Motee, "Wide-area control of power networks with time-delay," *IFAC*, vol. 51, no. 23, pp. 277 – 282, 2018.
[13] E. Ekomwenrenren, H. Alharbi, T. Elgorashi, J. Elmirghani, and P. Aristidou, "Stabilising control strategy for cyber-physical power systems," *IET Cyber-Physical Systems: Theory & Applications*, 2019.
[14] J. M. Thangaiah and R. Parthasarathy, "Delay-dependent stability analysis of power system considering communication delays," *International Trans. on Electrical Energy Sys.*, vol. 27, no. 3, 2017.
[15] E. Fridman, "Tutorial on Lyapunov-based methods for time-delay systems," *European Journal of Control*, vol. 20, no. 6, pp. 271 – 283, 2014.
[16] ——, *Introduction to Time-Delay Systems: Analysis and Control*. Birkhäuser, 2014.
[17] J. P. Hespanha, P. Naghshtabrizi, and Y. Xu, "A survey of recent results in networked control systems," *Proc.of the IEEE*, vol. 95, no. 1, pp. 138–162, 2007.
[18] H. K. Khalil, *Nonlinear systems*. Prentice Hall, 2002, vol. 3.
[19] J. Li, Z. Chen, D. Cai, W. Zhen, and Q. Huang, "Delay-dependent stability control for power system with multiple time-delays," *IEEE Trans. Power Syst.*, vol. 31, no. 3, pp. 2316–2326, 2016.
[20] S. Wang, X. Meng, and T. Chen, "Wide-area control of power systems through delayed network communication," *IEEE Trans. Control Syst. Technol.*, vol. 20, no. 2, pp. 495–503, 2012.
[21] B. Yang and Y. Sun, "Damping factor based delay margin for wide area signals in power system damping control," *IEEE Trans. Power Syst.*, vol. 28, no. 3, pp. 3501–3502, 2013.
[22] S. Qiang, A. Haiyun, J. Hongjie, Y. Xiaodan, W. Chengshan, W. Wei, M. Zhiyu, Z. Yuan, Z. Jinli, and L. Peng, "An improved power system stability criterion with multiple time delays," in *IEEE PES General Meeting*, 2009.
[23] U. Markovic, O. Stanojev, E. Vrettos, P. Aristidou, D. Callaway, and G. Hug, "Understanding Stability of Low-Inertia Systems," *IEEE Transactions on Power Systems*, (under review). [Online]. Available: engrxiv.org/jwzrq
[24] A. Fuchs, M. Imhof, T. Demiray, and M. Morari, "Stabilization of large power systems using VSC–HVDC and model predictive control," *IEEE Trans. Power Del.*, vol. 29, no. 1, pp. 480–488, 2014.
[25] M. Singh, A. Allen, E. Muljadi, and V. Gevorgian, "Oscillation damping: A comparison of wind and photovoltaic power plant capabilities," in *IEEE PEMWA*, 2014.
[26] L. Zacharia, L. Hadjidemetriou, and E. Kyriakides, "Integration of renewables into the wide area control scheme for damping power oscillations," *IEEE Trans. Power Syst.*, vol. 33, no. 5, 2018.
[27] C. Liu, G. Cai, W. Ge, D. Yang, C. Liu, and Z. Sun, "Oscillation analysis and wide-area damping control of DFIGs for renewable energy power systems using line modal potential energy," *IEEE Trans. Power Syst.*, vol. 33, no. 3, pp. 3460–3471, 2018.
[28] X. Wu, F. Dörfler, and M. R. Jovanović, "Input-output analysis and decentralized optimal control of inter-area oscillations in power systems," *IEEE Trans. Power Syst.*, vol. 31, no. 3, pp. 2434–2444, 2016.
[29] A. Mešanović, U. Münz, J. Bamberger, and R. Findeisen, "Controller tuning for the improvement of dynamic security in power systems," in *2018 IEEE PES ISGT-Europe*, 2018.

[30] M. Li and Y. Chen, "A wide-area dynamic damping controller based on robust $\mathcal{H}_\infty$ control for wide-area power systems with random delay and packet dropout," *IEEE Trans. Power Syst.*, vol. 33, no. 4, 2018.
[31] A. Seuret, F. Gouaisbaut, and E. Fridman, "Stability of systems with fast-varying delay using improved Wirtinger's inequality," in *52nd IEEE CDC*, 2013, pp. 946–951.
[32] C. A. R. Crusius and A. Trofino, "Sufficient LMI conditions for output feedback control problems," *IEEE Trans. Autom. Control*, vol. 44, no. 5, pp. 1053–1057, 1999.
[33] S. Alghamdi, J. Schiffer, and E. Fridman, "Distributed secondary frequency control design for microgrids: Trading off l_2-gain performance and communication efforts under time-varying delays," in *European Control Conference (ECC)*, 2018, pp. 758–763.
[34] U. Markovic, J. Vorwerk, P. Aristidou, and G. Hug, "Stability analysis of converter control modes in low-inertia power systems," in *IEEE ISGT-Europe*, 2018.
[35] R. Ofir, U. Markovic, P. Aristidou, and G.Hug, "Droop vs. virtual inertia: Comparison from the perspective of converter operation mode," in *2018 IEEE ENERGYCON*, 2018.
[36] ENTSO-E, "Documentation on controller tests in test grid configurations," Tech. Rep., 2013.
[37] P. M. Anderson and A. A. Fouad, *Power system control and stability*. John Wiley & Sons, 2008.
[38] J. Schiffer, D. Zonetti, R. Ortega, A. M. Stanković, T. Sezi, and J. Raisch, "A survey on modeling of microgrids—from fundamental physics to phasors and voltage sources," *Automatica*, vol. 74, pp. 135–150, 2016.
[39] P. Kokotovic, H. K. Khali, and J. O'reilly, *Singular perturbation methods in control: analysis and design*. Siam, 1999, vol. 25.
[40] P. Vorobev, P. Huang, M. A. Hosani, J. L. Kirtley, and K. Turitsyn, "High-fidelity model order reduction for microgrids stability assessment," *IEEE Trans. Power Syst.*, vol. 33, no. 1, pp. 874–887, 2018.
[41] I. Caduff, U. Markovic, C. Roberts, G. Hug, and E. Vrettos, "Reduced-Order Modeling of Inverter-Based Generation using Hybrid Singular Perturbation," in *2020 Power Systems Computation Conference (PSCC)*.
[42] J. Schiffer, E. Fridman, R. Ortega, and J. Raisch, "Stability of a class of delayed port-hamiltonian systems with application to microgrids with distributed rotational and electronic generation," *Automatica*, vol. 74, pp. 71–79, 2016.
[43] J. Schiffer, F. Dörfler, and E. Fridman, "Robustness of distributed averaging control in power systems: Time delays & dynamic communication topology," *Automatica*, vol. 80, pp. 261–271, 2017.
[44] S. Alghamdi, J. Schiffer, and E. Fridman, "Conditions for delay-robust consensus-based frequency control in power systems with second-order turbine-governor dynamics," in *CDC*, 2018, pp. 786–793.
[45] J. Löfberg, "YALMIP : a toolbox for modeling and optimization in matlab," in *IEEE International Conf. on Robotics & Automation*, 2004.
[46] M. ApS, *The MOSEK optimization toolbox for MATLAB manual. Version 8.1.0.51*, 2017.

APPENDIX

Proof of Proposition III.2. The proof is based on a combination of the stability analysis conducted in [31] with the control design approach using the descriptor method in [16] and the change of variables proposed in [32]. Consider the positive definite augmented LKF [31]

$$V(x_s,\dot{x}_s,t) = V_1 + V_2 + V_3, \tag{12}$$

where

$$V_1 = \begin{bmatrix} x_s \\ \int_{t-h_1}^{t} x_s(s)ds \\ \int_{t-h_2}^{t-h_1} x_s(s)ds \end{bmatrix}^\top P \begin{bmatrix} x_s \\ \int_{t-h_1}^{t} x_s(s)ds \\ \int_{t-h_2}^{t-h_1} x_s(s)ds \end{bmatrix},$$

$$V_2 = \int_{t-h_1}^{t} x_s^\top(s)S_1x_s(s)ds + \int_{t-h_2}^{t-h_1} x_s^\top(s)S_2x_s(s)ds,$$

$$V_3 = h_1\int_{-h_1}^{0}\int_{t+\phi}^{t} \dot{x}_s^\top(s)R_1\dot{x}_s(s)dsd\phi + h_{12}\int_{-h_2}^{-h_1}\int_{t+\phi}^{t} \dot{x}_s^\top(s)R_2\dot{x}_s(s)dsd\phi,$$

where $P>0$, $S_1>0$, $S_2>0$, $R_1>0$, and $R_2>0$ and $h_{12}=h_2-h_1$, see (7). Then, by invoking [16, Lemma 4.3], the design objectives in Problem III.1 are equivalent to the following constraint optimization problem

$$\begin{aligned} &\min \gamma \\ &\text{subject to} \\ &\dot{V}(x_s,\dot{x}_s,t) - \left(\gamma^2\|w(t)\|_2^2 - \|z(t)\|_2^2\right) \leq \\ &-\varrho\left(\|x_s(t)\|_2^2 + \|w(t)\|_2^2\right), \end{aligned}$$

where $\dot{V}$ denotes the time-derivative of the LKF V in (V), $\|\cdot\|_2$ is the Euclidean norm and ϱ is some positive constant.

As shown in [31], the differentiation of V along the trajectories of the system (6) yields

$$\dot{V} = \dot{V}_1 + \dot{V}_2 + \dot{V}_3, \tag{13}$$

with

$$\begin{aligned} \dot{V}_1 = &\begin{bmatrix} x_s \\ \int_{t-h_1}^{t} x_s(s)ds \\ \int_{t-h_2}^{t-h_1} x_s(s)ds \end{bmatrix}^\top P \begin{bmatrix} \dot{x}_s \\ x_s - x_s(t-h_1) \\ x_s(t-h_1) - x_s(t-h_2) \end{bmatrix} \\ &+ \begin{bmatrix} \dot{x}_s \\ x_s - x_s(t-h_1) \\ x_s(t-h_1) - x_s(t-h_2) \end{bmatrix}^\top P \begin{bmatrix} x_s \\ \int_{t-h_1}^{t} x_s(s)ds \\ \int_{t-h_2}^{t-h_1} x_s(s)ds \end{bmatrix}, \end{aligned}$$

$$\begin{aligned} \dot{V}_2 =& x_s^\top(t)S_1x_s(t) - x_s^\top(t-h_1)S_1x_s(t-h_1) \\ &+ x_s^\top(t-h_1)S_2x_s(t-h_1) - x_s^\top(t-h_2)S_2x_s(t-h_2), \\ \dot{V}_3 =& h_1^2\dot{x}_s^\top(t)R_1\dot{x}_s(t) + h_{12}^2\dot{x}_s^\top(t)R_2\dot{x}_s(t) \\ &-h_1\int_{t-h_1}^{t} \dot{x}_s^\top(s)R_1\dot{x}_s(s)ds - h_{12}\int_{t-h_2}^{t-h_1} \dot{x}_s^\top(s)R_2\dot{x}_s(s)ds. \end{aligned}$$

Inspired by [31], we introduce the vector

$$\begin{aligned} \zeta(t) = \Big[&x_s^\top(t), \dot{x}_s^\top(t), x_s^\top(t-h_1), x_s^\top(t-\tau), x_s^\top(t-h_2), \\ &\frac{1}{h_1}\int_{t-h_1}^{t} x_s^\top(s)ds, \frac{1}{\tau-h_1}\int_{t-\tau}^{t-h_1} x_s^\top(s)ds, \\ &\frac{1}{h_2-\tau}\int_{t-h_2}^{t-\tau} x_s^\top(s)ds, w^\top\Big]^\top. \end{aligned} \tag{14}$$

Then, by using G_0 and $G_1(\tau)$ from (7), we obtain

$$\begin{aligned} \begin{bmatrix} x_s \\ \int_{t-h_1}^{t} x_s(s)ds \\ \int_{t-h_2}^{t-h_1} x_s(s)ds \end{bmatrix} =& G_1(\tau)\zeta(t), \\ \begin{bmatrix} \dot{x}_s \\ x_s - x_s(t-h_1) \\ x_s(t-h_1) - x_s(t-h_2) \end{bmatrix} =& G_0\zeta(t) \end{aligned} \tag{15}$$

and $\dot{V}_1$ can be compactly written as

$$\dot{V}_1 = \zeta^\top \left(G_0^\top P G_1(\tau) + G_1^\top(\tau) P G_0 \right) \zeta. \tag{16}$$

Next, consider $\dot{V}_3$ in (14). Applying the improved integral inequality, i.e., [31, Lemma 2.1] gives

$$\begin{aligned} &- h_1 \int_{t-h_1}^{t} \dot{x}_s^\top(s) R_1 \dot{x}_s(s) ds \leq \\ &- \begin{bmatrix} x_s - x_s(t-h_1) \\ x_s + x_s(t-h_1) - \frac{2}{h_1} \int_{t-h_1}^{t} x_s(s) ds \end{bmatrix}^\top \begin{bmatrix} R_1 & \mathbb{0} \\ \mathbb{0} & 3R_1 \end{bmatrix} \\ &\begin{bmatrix} x_s - x_s(t-h_1) \\ x_s + x_s(t-h_1) - \frac{2}{h_1} \int_{t-h_1}^{t} x_s(s) ds \end{bmatrix}. \end{aligned} \tag{17}$$

Furthermore, as shown in [31], combining [31, Lemma 2.1] and [31, Lemma 2.2] allows to obtain

$$- h_{12} \int_{t-h_2}^{t-h_1} \dot{x}_s^\top(s) R_2 \dot{x}_s(s) ds \leq -\zeta^\top \Gamma^\top \psi_2 \Gamma \zeta, \tag{18}$$

where Γ is given in (7), X is a matrix variable and

$$\psi_2 = \begin{bmatrix} \hat{R}_2 & X \\ * & \hat{R}_2 \end{bmatrix}, \quad \hat{R}_2 = \begin{bmatrix} R_2 & 0 \\ 0 & 3R_2 \end{bmatrix}. \tag{19}$$

Then, differently from the analysis conditions presented in [31], for the purpose of deriving a controller synthesis we employ the descriptor method, see [16, Chapter 3]. Let P_2 and P_3 be matrix variables and introduce the following expression

$$0 = 2 \left[x_s^\top P_2^\top + \dot{x}_s^\top P_3^\top \right] \left[A x_s - B_u K C_y x_s(t-\tau) + B_w w - \dot{x}_s \right]. \tag{20}$$

Then, summing up (20), (16), $\dot{V}_2$, the first two terms in $\dot{V}_3$ in (14) and (18), considering the output performance z in (6) and following the procedure in [16, Section 4.3.2] gives

$$\begin{aligned} &\dot{V}(x_s, \dot{x}_s, t) - \left(\gamma^2 \|w(t)\|_2^2 - \|z(t)\|_2^2 \right) \leq \\ &\zeta^\top \left(\psi_{11} + G_0^\top(\tau) P G_1 + G_1^\top P G_0(\tau) - \Gamma^\top \psi_3 \Gamma + \psi_2^\top \psi_2 \right) \zeta, \end{aligned} \tag{21}$$

where ζ is given in (14), ψ_{11} is defined in (22), $G_0(\tau)$, G_1 and Γ are given in (7), ψ_3 is defined in (19) and $\psi_2^\top = [C_z, \mathbb{0}, \mathbb{0}, -D_u K C_y, \mathbb{0}, \mathbb{0}, \mathbb{0}, \mathbb{0}, D_w]$. The right hand-side of (21) being negative for $\zeta \neq \mathbb{0}$ is, by using the Schur complement [16], equivalent to

$$\begin{bmatrix} \psi_1(\tau) & \psi_2 \\ * & -I \end{bmatrix} < 0. \tag{23}$$

where $\psi_1 = \psi_{11} + G_0^\top(\tau) P G_1 + G_1^\top P G_0(\tau) - \Gamma^\top \psi_3 \Gamma$.

Due to the terms $P_2^\top B_u K C_y$ and $P_3 B_u K C_y$, the matrix ψ_{11} in (22) is bilinear in the decision variables P_2, P_3 and K. To overcome this drawback, we choose

$$P_3 = \epsilon P_2, \quad W = P_2^{-1}, \tag{24}$$

where ϵ is a tuning scalar. Then, we perform a congruence transformation on the matrix in (23) by multiplying it by $\mathrm{diag}(W, W, W, W, W, W, W, W, I, I)$ and its transpose from the right and left, respectively. We also define the matrices

$$\begin{aligned} [\bar{S}_1, \bar{S}_2, \bar{R}_1, \bar{R}_2] &= W^\top [S_1, S_2, R_1, R_2] W, \\ \bar{P} &= \mathrm{diag}(W, W, W)^\top P \, \mathrm{diag}(W, W, W), \\ \bar{X} &= \mathrm{diag}(W, W)^\top X \, \mathrm{diag}(W, W) \end{aligned} \tag{25}$$

and, following [32, W-Problem], introduce new matrix variables M and N satisfying

$$M C_y = C_y W, \quad K = N M^{-1}. \tag{26}$$

By defining $\bar{\gamma} = \gamma^2$, we then obtain (7), which is a LMI in the auxiliary controller variables N and M as well as in the variables $\bar{\gamma}$, $\bar{P}$, $\bar{R}_1$, $\bar{R}_2$, $\bar{X}$, $\bar{S}_1$ and $\bar{S}_2$ with additional (fixed) tuning parameter ε.

Finally, since $\bar{\psi}_1(\tau)$ in (7) is affine with respect to τ, a necessary and sufficient condition for $\bar{\psi}_1(\tau) < 0$ for all $\tau \in [h_1, h_2]$ is that $\bar{\psi}_1(\tau = h_1) < 0$ and $\bar{\psi}_1(\tau = h_2) < 0$ hold simultaneously, see e.g. [31]. Hence, under the made assumptions, all conditions of [16, Lemma 4.3] are satisfied. This completes the proof.

□□□

$$\psi_{11} = \begin{bmatrix} P_2^\top A + A^\top P_2 + S_1 - 4R_1 & -P_2^\top + A^\top P_3 & -2R_1 & -P_2^\top B_u K C_y & \mathbb{0} & 6R_1 & \mathbb{0}\,\mathbb{0} & P_2^\top B_w \\ * & -P_3^\top - P_3 + h_1^2 R_1 + h_{12}^2 R_2 & \mathbb{0} & -P_3^\top B_u K C_y & \mathbb{0} & \mathbb{0} & \mathbb{0}\,\mathbb{0} & P_3^\top B_w \\ * & * & -S_1 + S_2 - 4R_1 & \mathbb{0} & \mathbb{0} & 6R_1 & \mathbb{0}\,\mathbb{0} & \mathbb{0} \\ * & * & * & \mathbb{0} & \mathbb{0} & \mathbb{0} & \mathbb{0}\,\mathbb{0} & \mathbb{0} \\ * & * & * & * & -S_2 & \mathbb{0} & \mathbb{0}\,\mathbb{0} & \mathbb{0} \\ * & * & * & * & * & -12R_1 & \mathbb{0}\,\mathbb{0} & \mathbb{0} \\ * & * & * & * & * & * & \mathbb{0}\,\mathbb{0} & \mathbb{0} \\ * & * & * & * & * & * & *\,\mathbb{0} & \mathbb{0} \\ * & * & * & * & * & * & *\,* & -\gamma^2 I \end{bmatrix} \tag{22}$$